ESI_5-Clasp1. Supporting Information for paper:-

Experimental and theoretical investigations of the polymorphism of 5-chloroacetoxybenzoic acid (5-chloroaspirin)

Riccardo Montis[a], Michael B. Hursthouse[a,c*], H. C. Stephen Chan[b], John Kendrick[b] and Frank J. J. Leusen[b*]

[a] School of Chemistry, University of Southampton, Southampton, SO17 1BJ, UK [b] School of Life Sciences, University of Bradford, Bradford, BD7 1DP, UK c) Department of Chemistry, Faculty of Science, Kin Abdulazziz University, Saudi Arabia.

This ESI component is essentially an appendix to the above paper, providing additional details of experimental crystallization, thermal, and spectroscopic studies and discusses in greater detail the relationships between some of the higher energy predicted 5-chloroaspirin structures and experimental structures. Also provided are geometrical details of the geometry parameters of the SC's identified and discussed.

A. Additional Experimental Detail

1. Crystallizations

Single crystals of both α and β forms of 5-chloro-2-acetoxysalicylic acid suitable for X-ray study were variously grown by evaporation from an extensive selection of pure and mixed solvents, see Table ESI 1. Slow evaporation tended to give the α form, rapid crystallization (generally with the more volatile solvents) gave mainly the β form. Both forms crystallize adopting various morphologies such as blade, prism and needle (Figure ESI 1). In particular samples from Toluene (5-Cl α) and DCM (5-Cl β) crystallize adopting the same crystal habit (Figure ESI 2).

Table ESI 1. Crystallizations of 5-Cl α and 5-Cl β from various solvents.[a]

Solvents	5-Cl (α)	5-Cl (β)
methanol	√	√
ethanol	√	√
acetonitrile	√	√
nitromethane	√	√
acetone	√	√
methanol /H_2O 1:1	√	-
ethanol /H_2O 1:1	√	√
acetonitrile /H_2O 1:1	√	√
2-propanol	√	√
acetone/H_2O 1:1	√	√
acetone/acetonitrile 1:1	√	-
Toluene	√	-
chloroform	√	√
ethyl acetate	√	√
dichloromethane	√	√
tetrahydrofurane	√	√

[a]A succesful crystallization experiment is indicated by the √ symbol.

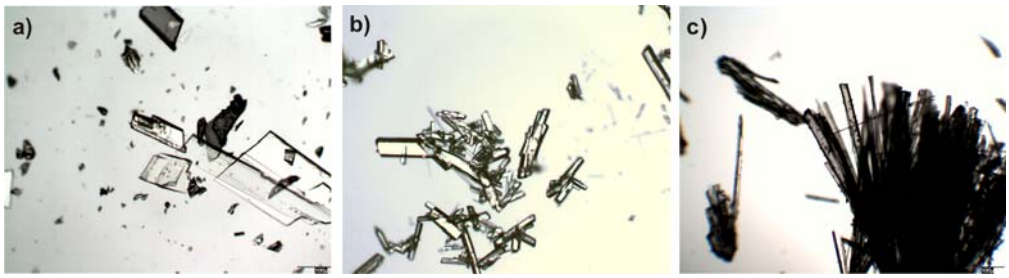

Figure ESI 1. Various crystal habits for 5-Cl α and 5-Cl β. a) blade; b) prism; c) needle.

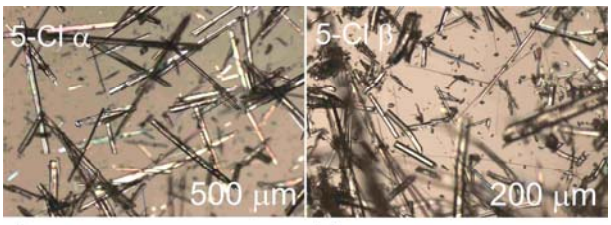

Figure ESI 2. Crystal habits for a) 5-Cl α (from toluene) and b) 5-Cl β (from DCM).

2. IR Spectroscopic and Thermal Methods Investigations

Newly obtained crystalline samples were normally checked via Differential Scanning Calorimetry experiments and Infrared spectroscopy. Several samples prepared initially had DSC curves and FT-IR spectra which were consistent with clean products. Initially, melting points were recorded with peak values of about 151.6 ± 0.8 for the α form and 147.0 ± 0.2 for the β form. However further analysis revealed samples with higher melting points, with the presence of extra peaks at approximately 130 °C (Figure ESI 3).

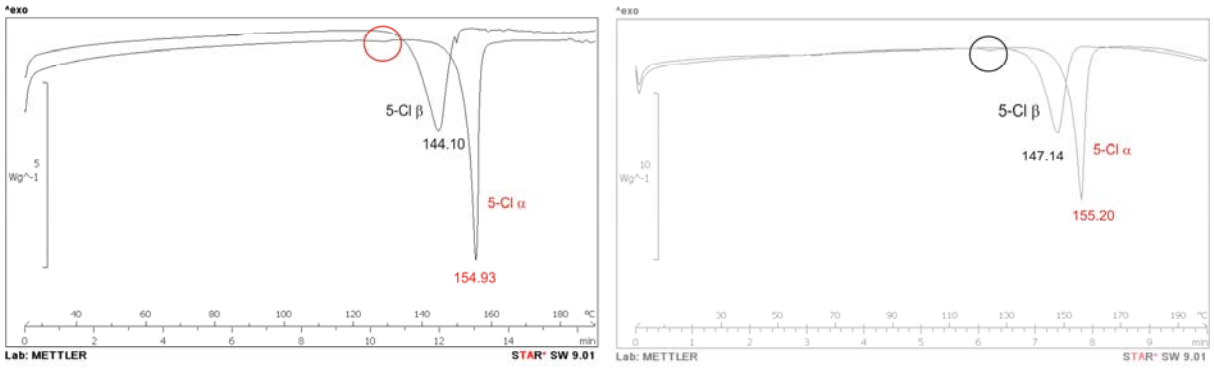

a) b)

Figure ESI 3. DSC curves showing the peak at approximately 130 °C (a) for 5-Cl α (red) and (b) 5-Cl β (black). The curves are collected at different heating rate: a) temperature range 0-200 at 10 °C / min; b) temperature range 0-200 at 20 °C / min.

This behavior was observed for both 5-Cl α and 5-Cl β samples. As described in the main paper the hot-stage analysis excluded any phase transition occurring in the two polymorphs. One possible explanation for this occurrence may be the presence of impurities of 5-chlorosalicylic acid in the samples. This possibility was further investigated. In particular, a comparison of the FT-IR of some samples of 5-Cl α, 5-Cl β and pure 5-chlorosalicylic acid (5-ClSA) as shown in Figure ESI 4 confirmed that the salicylic acid impurities are present in some of the 5-Cl α and 5-Cl β samples. These impurities might derive from a decomposition process or directly from the synthesis. Salicylic acid impurities may actually form a eutectic with a melting temperature around 130 °C.

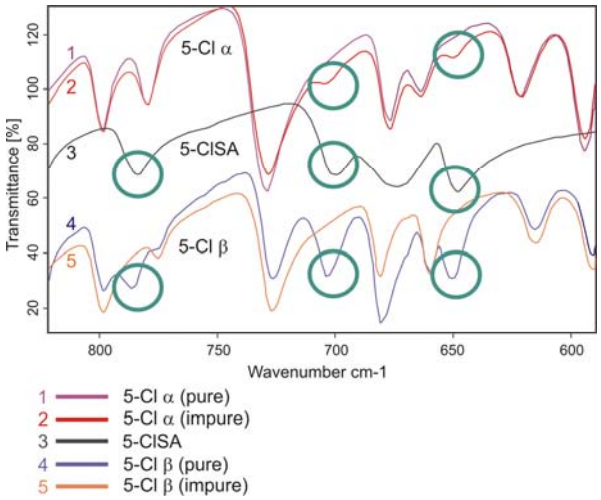

Figure ESI 4. Comparison of the FT-IR spectra of 5-chlorosalicylic acid (5-ClSA) and pure and impure samples of the two polymorphs. Green circles indicate the peaks deriving from the impurities of 5-ClSA.

This was confirmed by an HSM analysis using the "contact method"[1] procedure, which demonstrated that 5-ClAsp in the presence of 5-ClSA (M.P. = 170°C) forms an eutectic mixture which melts at approximately 130 °C as observed in some DSC curves. Figure ESI 5 shows the two components, 5-ClAsp (on the left side) and 5-ClSA (on the right side), separated by the contact surface. At 129-130 °C melting occurs at the contact surface indicating that the melting point of the eutectic mixture lies within this range of temperatures.

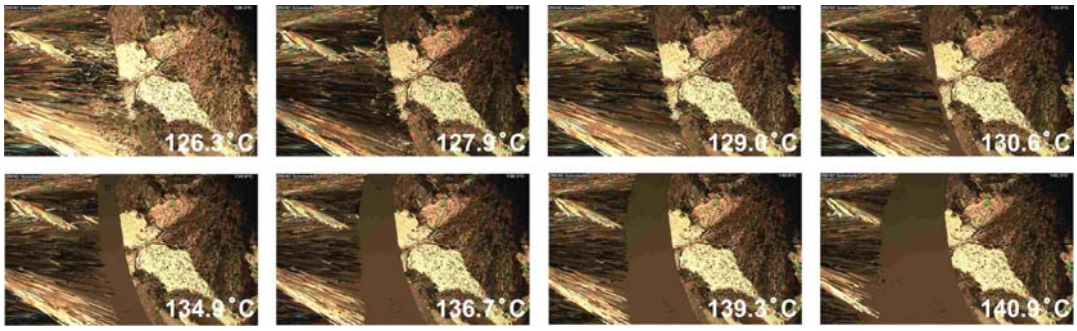

Figure ESI 5. HSM analysis of the eutectic mixture obtained by recrystallizing from the melt of 5-ClAsp (left side of each image) and 5-ClSA (right side of each image).

The above results are important in the context of further uncertainties, which came to light during a major screening experiment made in order to search for further polymorphs. In the screening results, products were predominantly of the β form and in some cases an increase in the melting point was noticed, to the extent that some values were greater than that originally obtained for the α form. Accordingly attention was refocused on recrystallizing new samples of each form by careful, slow evaporation. Finally, what seemed to be reliable samples of

each form were obtained, as shown by DSC and FT-IR, plus powder X-ray diffraction (PXRD). For the latter, a Bruker GADDS diffractometer and software were used (see below) which allowed examination of samples which were not crushed or powderised. The samples used were those also used for the definitive DSC and FT-IR measurements recorded in the main paper.

The PXRD measurements were carried out on a Bruker GADDS combinatorial X-ray instrument equipped with an XYZ stage and a Multi-wire Hi-Star area detector. Small amounts of unground sample were placed on a glass slide, the patterns recorded and integrated using the GADDS/Eva software.[2]

For the PXRD, the following settings were used:

Radiation: Cu Kα; **Monochromator:** Göbel Mirror;

Collimator: Long, 0.5 mm; **Pre collimator slit:** 1.0 mm; **Detector Distance:** 15 cm;

Theta 1 (Tube Arm): 11.65°; **Theta 2 (Detector Arm):** 11.65°;

Time: 600 seconds (10 minutes); **Software:** GADDS/Eva;

Integration type: Chi Integrate, range -111.200 , -65.5; 2theta range 6.100 – 40.9;

Conditions: Ambient;

Calibration: The calibration of the instrument was checked before each set of samples was run using the NIST Corundum Standard Reference Material SR1976 and found to be correct within 0.1 degree.

The patterns obtained are given in Figure ESI 6, which show that, bearing in mind the nature of the samples, each form seems to be clear of any observable amount of the other form, with peaks having significant intensities in each pattern but not present in the other.

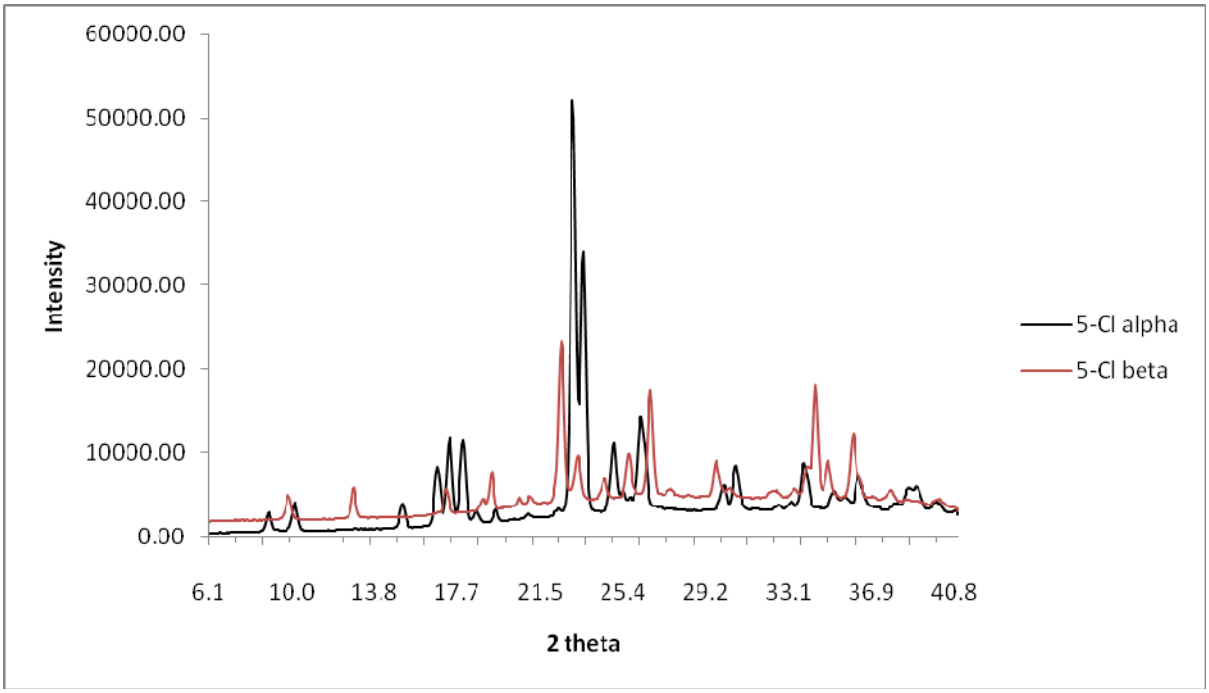

Figure ESI 6. Powder diffraction patterns for 5-Cl α (black) and 5-Cl β (red)

The fundamental origin(s) of the shifting melting points are uncertain. Melting points may often be reduced by impurities or defects, but variations in melting points could also be due to intergrowth of one polymorph in the other. However, these should show up on the single crystal diffraction patterns, and no such features were noticed for our samples which were used to obtain single crystal data. This is mentioned here because of the involvement of such effects in the growth of the two forms of pure aspirin.[3-5] In the present case, however, microscopic occurrences of one form could be envisaged in a crystal of the other, as a result of the 2-D similarity between the structures, but with regions too small to give any significant contributions to the major diffraction pattern. We plan to investigate this situation in the future.

B. Further discussion of the detailed XPac Analysis

First of all, we present here more detailed discussion of the three Supramolecular Constructs which contain the 1-D Construct AB1, namely AB21, AB22 and AB23. Figure ESI 7 shows an alternative view of the 2-D AB21 construct which comprises a corrugated **t2/t3** layer of side-by-side AB1 chains, as they occur in the structures of 5-Cl β and 5-Cl 10, with the chains in each construct geometrically related by glide symmetry (the orange or blue

components of Figure ESI 7 a and b each represent one instance of AB21). The constructs sit atop similar ones stacking up in the **t1** direction to build up the 3-D structure. Molecules in the stacks are connected vertically by different C-H···O interactions, as shown, but the AB1 chains forming the AB21 layer construct are connected via the (phenyl)-C-H4···O4-(acetyl) interactions in a partially stepped manner. As indicated in Figure 7 in the main paper, this construct and relationship is common for the isostructural set 5-Cl β, 5-MeO and 5-Cl 05, and also for 5-Cl 10. This construct is specifically identified because structure 5-Cl 10 was separated from the others.

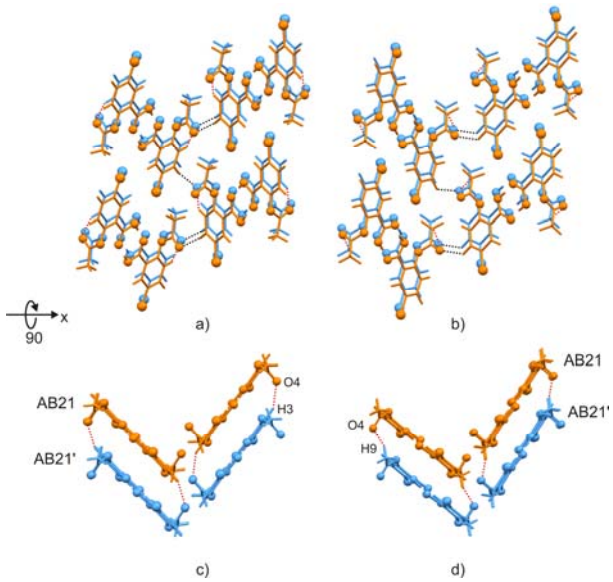

Figure ESI 7. 2-D Supramolecular Construct (SC) AB21 shown for 5-Cl β (a) and 5-Cl 10 (b) viewed along approximately the stacking direction and its perpendicular direction (c and d). Different instances are represented by different colors: orange (AB21) and blue (AB21').

However, if more generous filter parameters are used for the comparison, the division is lost and all structures show a 3-D similarity by incorporating the loosely similar stacking arrangements of the 5-Cl β set and 5-Cl 10. This similarity accommodates the shifts and tilting of the molecules in the stacking development which involves C-H···O intermolecular interactions between the acetyl carbonyl O(4) and respectively the aromatic H(9) for the isostructural set, and the acetyl methyl H(3) for the predicted structure 5-Cl 10 (Figure ESI 8 a-d). However, the angles formed by the base vectors differ as in the previous examples by about 20°. Notwithstanding this finding, it was decided to retain the separation between the 5-Cl β, 5-MeO, 5-Cl 05 isostructural set and 5-Cl 10 as indicated in Figure 7 in the main paper. The reason for this decision is amplified in the following paragraph.

The second 2-D SC, labelled AB22, comprises stacks of AB1 chains (see Figure ESI 8). It involves prediction 5-Cl 10, but now linked with the isostructural set 5-Cl α, 5-Br, 5-I, 5-Cl 02 and 5-Cl 04, and not the 5-Cl β, 5-MeO and 5-Cl 05 set, with which it shares the same geometry and C-H···O interactions. The slippages and tilts in the stacks are now very similar, each with a **t1**/**t2** angle of 90°. However, the sewing together of the stacks shows the same symmetry difference as in the experimental pair 5-Cl α and 5-Cl β (see Figure ESI 8). The net result of these relationships is that predicted form 5-Cl 10 has the same stacking of AB1 chains found in 5-Cl α but the side-by-side stitching found in 5-Cl β. This result suggests that the earlier assumption, proposed in the main paper, that the stacking differences were linked to the stitching symmetry of the stacks may not be the full story. It is intriguing, therefore, to consider why the CSP calculation "crystallized" 5-Cl 10 into what may be a local minimum, and whether this might have any implications for real structures.

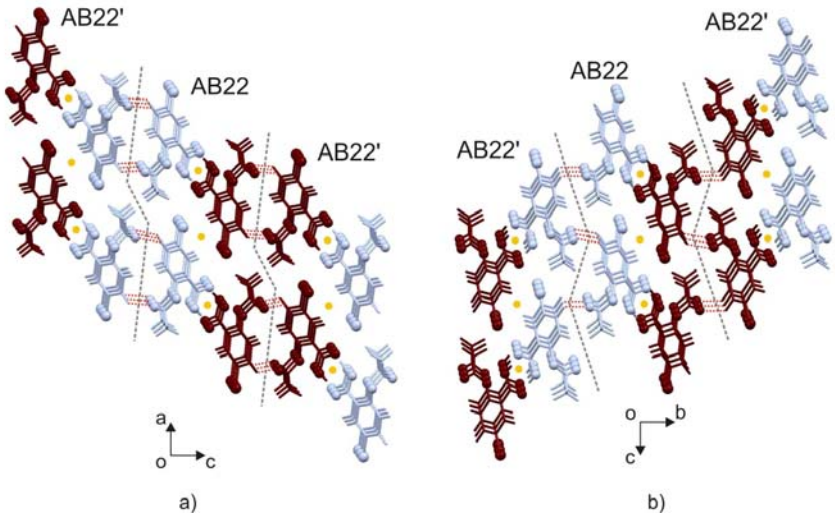

Figure ESI 8. 2-D Supramolecular Construct (SC) AB22: a) 5-Cl α and b) 5-Cl 10. The molecules are color coded according to the direction of the ring-carboxylate vector: red pointing towards the viewer, blue pointing away. Different instances of the SC (AB22 and AB22') and the interactions involved in connecting each other are also represented.

It can be assumed, for example, that if the predicted polymorph 5-Cl 10 could exist, it might convert to 5-Cl β/5-Cl 05 with a small shift in the stacking arrangement coupled with a re-arrangement of the set of intra-stack C-H···O interactions. Most importantly, however, a transformation of the carboxylate isomer form would also be required.

AB23 is a further 2-D SC common to the three pairs of predicted isostructures 5-Cl 01-03, 5-Cl 08-12 and 5-Cl 09-11 (see Figure ESI 9). This arrangement again consists of stacks of

chains AB1 very similar to AB22, but differing in the shifting of adjacent molecules along the stacking direction (see below). More significantly, however, the 3-D structures show very significant differences in the way in which the stacks are sewn together, in spite of the fact that the same C-H···O intermolecular interactions between the acetyl carbonyl O(4) and the aromatic H(3) are used. The differences are mainly concerned with the symmetry operations which relate the neighboring instances of SC AB23 (blue and dark blue in Figure ESI 9). In 5-Cl 01 (Figure ESI 9 a) the two instances of AB23 (AB23 and AB23') are related by centres of inversion. In 5-Cl 08, AB23 and AB23' are related by vertical 2_1 screw axes lying between the acetyl groups. 5-Cl 09 (Figure ESI 9 c) shows a similar behavior as 5-Cl 01 but with some differences involving shifting along the *100* direction.

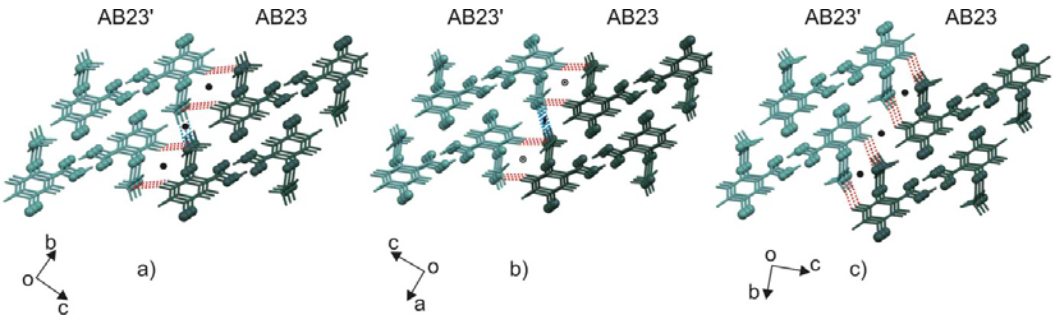

Figure ESI 9. 2-D Supramolecular Construct (SC) AB23: a) 5-Cl 01; b) 5-Cl 08; c) 5-Cl 09. Different instances (AB23 and AB23') and the interactions involved in connecting each other are also represented (C-H(3)···O(4) as red dashed lines; C-H(9)···O(4) as blue).

The most significant variations in the association of the AB23 constructs in the three structures involve major differences in the interactions involving the acetyl group (Figure ESI 10). 5-Cl 01 shows a centrosymmetric acetyl dimer analogous to that previously observed for many of the substituted aspirin derivatives.[6] As a consequence of the 2_1 screw axis, 5-Cl 08 adopts an acetyl catemer similar in some extent to that observed for polymorph 2 of aspirin.[3-5] In 5-Cl 09 the acetyl group is only involved in forming intra-stack C-H···O interactions with the aromatic H(3) as described above.

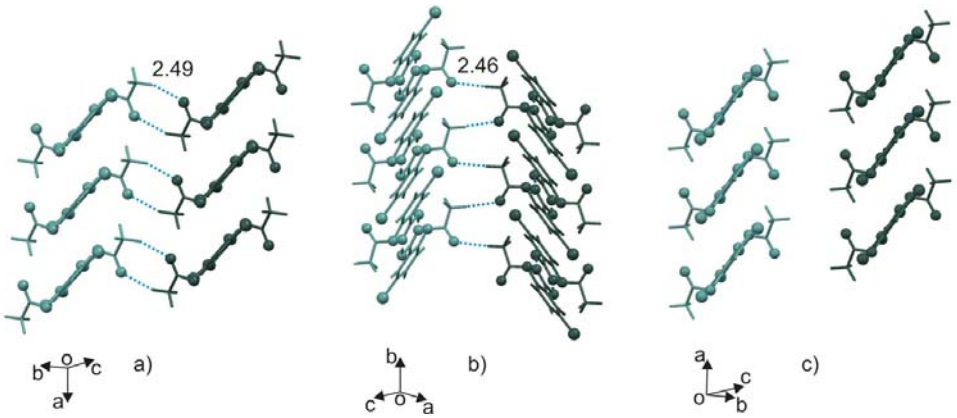

Figure ESI 10. Acetyl C-H···O involved in connecting different instances of the 2-D Supramolecular Construct (SC) AB23: a) 5-Cl 01; b) 5-Cl 08; c) 5-Cl 09.

Similarly to observations for the previous 2-D arrangements, the angles between the base vectors differ significantly (90° for AB22 and approximately 70° for AB23), indicating a third type of stacking arrangement. This is also confirmed by the analysis of the intermolecular interactions involved in defining this arrangement which reveal, again, the role of the acetyl group in determining connections between the carboxylic dimers along the direction of the propagation of the stacks. As in the previous cases, the C-H···O interactions have an important role in defining the molecular arrangement. The only difference concerns the position of the hydrogen which in this case is the aromatic H(4). Figure ESI 11 shows a comparison of the three arrangements found in the 2-D SCs AB21, AB22 and AB23.

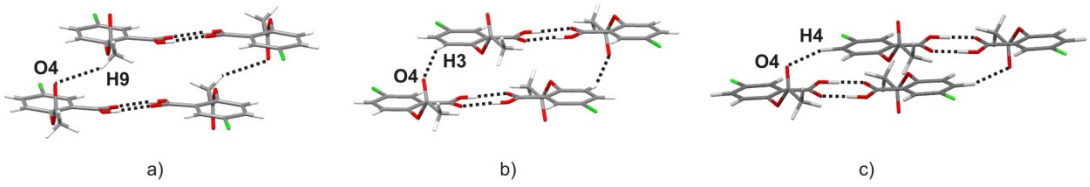

Figure ESI 11. Comparison of the interactions involved in the stacking motifs occurring in 5-Cl α (a); 5-Cl β (b) and 5-Cl 01 (c).

The last 2-D SC found is labelled as A21 and it is common for the isostructural pair of predicted structures 5-Cl 09-11 and aspirin form 1 (Asp 1). It consists of stacks of chains of carboxylic dimers connected via C-H···O between the acetyl carbonyl O(4) and the aromatic H(3). The two different 3-D structures are then built by different packing of the A21 constructs.

In Asp 1 the A21 constructs pack along the *001* direction related by the vertical 2_1 screw axis (Figure ESI 12 a), whereas in structures 5-Cl 09 and 5-Cl 11, A21 packs along the *100* direction by translation symmetry (Figure ESI 12 b).

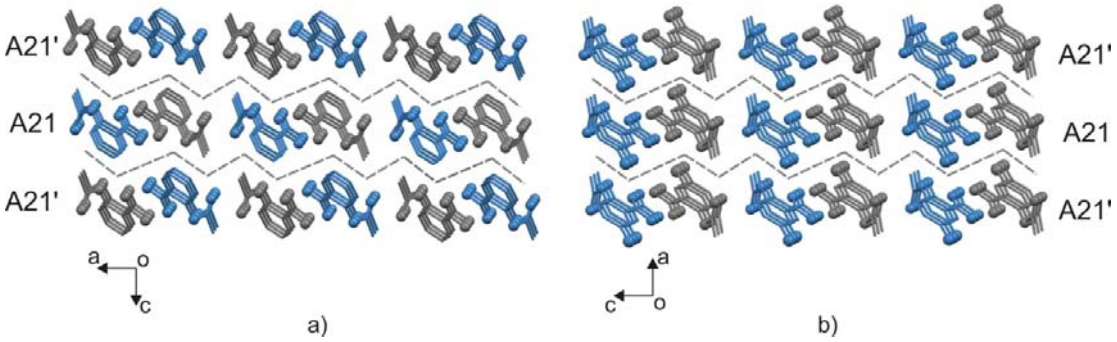

Figure ESI 12. 2-D Supramolecular Construct (SC) A21: a) Asp 1; b) 5-Cl 09. The molecules are color coded according to the direction of the ring-carboxylate vector: pointing towards the viewer (grey), pointing away from the viewer (blue).

Interestingly the second polymorph of aspirin, aspirin 2 (Asp 2), shows a 1-D similarity in common with the isostructural pair 5-Cl 01-03. This is labelled as 1-D SC A11 and consists of a zig-zag chain of carboxylic dimers related by inversion symmetry as shown in Figure ESI 13. No significant intermolecular interactions are involved in the development of the chains, indicating that this molecular arrangement derives from close packing. However 5-Cl 01 and 5-Cl 03 show C-H···O interactions between adjacent chains between the acetyl carbonyl O(4) and the acetyl methyl H(9).

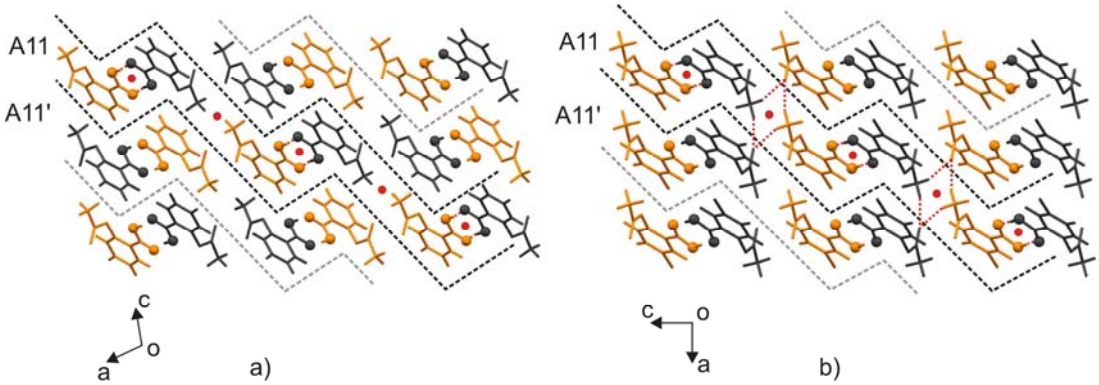

Figure ESI 13. 1-D Supramolecular Construct (SC) A11: a) Asp 2; b) 5-Cl 01. Different instances are separated by dashed lines. The molecules are color coded according to the direction of the ring-carboxylate vector: pointing towards the viewer (yellow), pointing away from the viewer (grey).

Using less strict filter parameters the Xpac analysis reveals a 2-D similarity which consists of stacks of the zig-zag chains described above. However the vectors along the stacking directions show a significant difference (approximately 1.2 Å) and the relationship between the structures is better described by a 1-D similarity. This is also confirmed by the comparison of the dissimilarity indices provided by the program which show a lower value for the 1-D similarity ($\chi_{1\text{-}D}$ = 5.9 and $\chi_{2\text{-}D}$ = 9.6 for Asp 2 and 5-Cl 01 as a representative).

The 1-D SC, F11, relates the set of three isostructural pairs 5-Cl 01-03, 5-Cl 08-12 and 5-Cl 09-11 and the 6-F derivative and consists of a row of single molecules (see Figure ESI 14) connected via C-H···O interactions involving the aromatic H(4) and the acetyl carbonyl O(4).

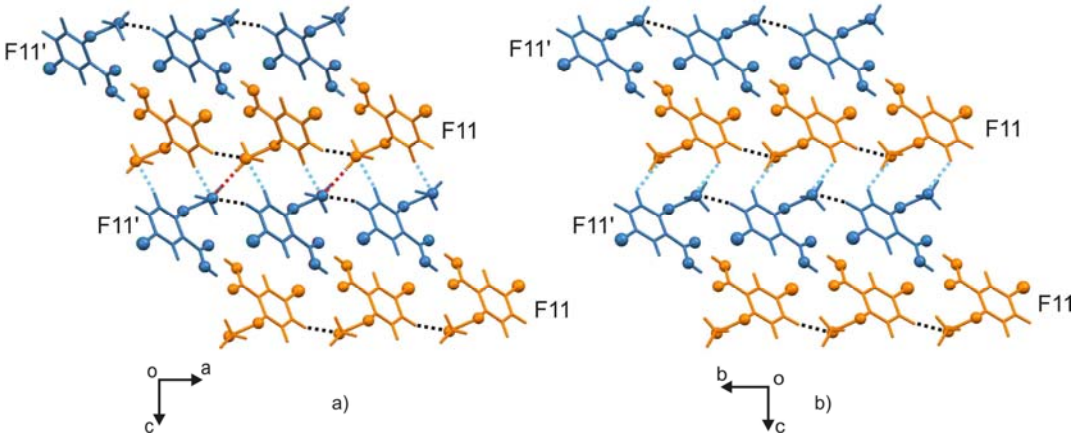

Figure ESI 14. 1-D Supramolecular Construct (SC) F11: a) 5-Cl 08; b) 5-Cl 09. Three different sets of interactions are identified: C-H(4)···O(4) (black), C-H(3)···O(4) (blue) and C-H(9)···O(4) (red). The molecules are color coded according to the direction of the ring-carboxylate vector: pointing towards the viewer (blue), pointing away from the viewer (yellow).

However, the pair 5-Cl 01-03 shows a further common arrangement with the 6-F derivative (6-FAsp) which contains the SC F11. This is the 1-D SC F12 (see Figure ESI 15) built by two adjacent rows of F11 related by inversion symmetry and connected by C-H···O interactions between the aromatic H(3) and the acetyl carbonyl O(4). This motif also identifies a new 0-D arrangement (Figure ESI 15 c) not reported in the relationship diagram since it occurs only in this higher dimension similarity.

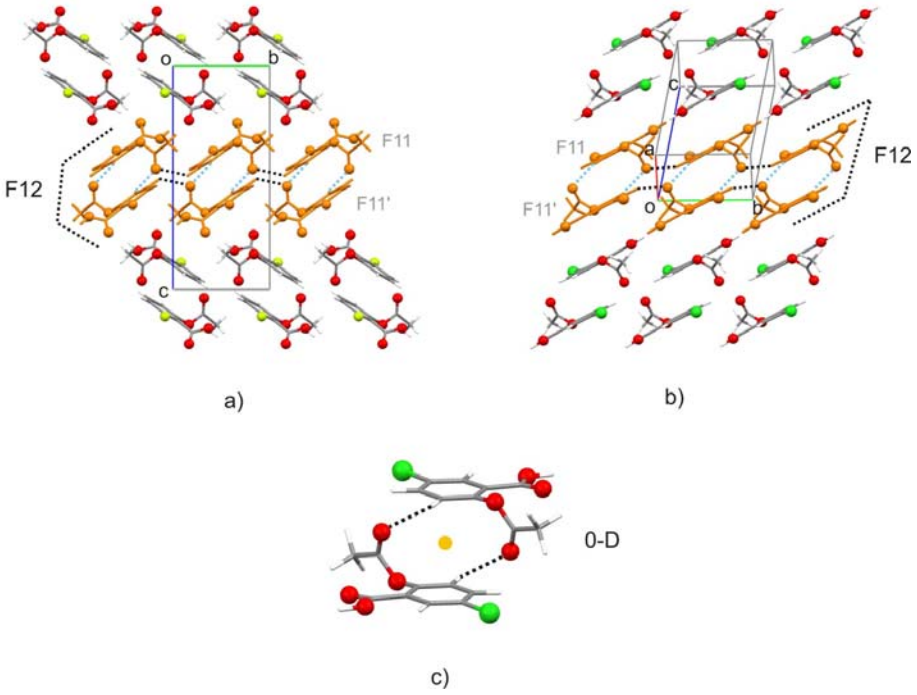

Figure ESI 15. 1-D Supramolecular Construct (SC) F12: a) 6-FAsp; b) 5-Cl 01; c) the precursor 0-D centrosymmetric dimer.

C. Supramolecular Constructs and Translational Vectors

Full details of the XPac Supramolecular Constructs and Translational Vectors are provided in Tables ESI 2 and ESI 3.

Table ESI 2. Supramolecular Construct descriptions.

SC[a]	D[b]	Description[c]	#[d]	Base[e]	Dependencies[f]
A1	0	Carboxylic acid dimer	28	-	-
B1	0	Carboxylic O···5-sub dimer	15	-	-
AB1	1	Tape- chain of A1 and B1 dimers > translation	15	t2	CP→A1, B1→ AB1
F11	1	Row of single molecules > translation	7	t4	CP→ F11
F12	1	sum of F11 rows > translation > inversion	3	t4	CP→ F11→ F12
A11	1	zig-zag chain of carboxylic dimers > inversion	3	t5	CP→A1→A11
AB21	2	corrugated layer of tilted AB1 chains > glide symmetry	4	t2,t3	CP→A1, B1→ AB1→ AB21
AB22	2	Stacks of AB1 chains > translation	6	t1,t2	CP→A1, B1→ AB1→ AB22
AB23	2	Slipped stacks of AB1 chains > translation	6	t6,t7	CP→A1, B1→ AB1→ AB23
A21	2	Stacks of zig-zag chain of carboxylic dimers > inversion >translation	3	t1,t5	A1→A11→A21
Isostructural		5-Cl 05, 5-Cl β; 5-Cl 02, 5-Cl 04, 5-Cl α; 5-Cl 08, 5-Cl 12; 5-Cl 01, 5-Cl 03; 5-Cl 09, 5-Cl 11; 5-Cl 06, 5-Cl 07			

[a]SC = Supramolecular Construct. [b]D = dimensionality. [c]'>' = is related by. [d]'#' = number of structures in which construct occurs. [e]Base = base vector of SC (see Table ESI 3).
[f]Dependencies show lower dimensionality SCs present in given SC.

Table ESI 3. Translational Vectors with lengths (Å). Grey color is used to indicate representative structures involved in Reference 2 of the Main Paper.

Structures	*t1*	d1	*t2*	d2	*t3*	d3	*t4*	d4	*t5*	d5	*t6*	d6	*t7*	d7	∠ (t2,t3)	∠ (t1,t2)	∠ (t6,t7)
5-Cl 01	-	-	110	10.832	-	-	010	7.669	10-1	13.004	100	5.698	010	7.669	-	-	72.65
5-Cl 02	010	4.756	100	10.216	-	-	-	-	-	-	-	-	-	-	-	90	-
5-Cl 03	-	-	110	10.656	-	-	010	7.570	101	13.181	100	5.637	010	7.570	-	-	73.33
5-Cl 04	010	4.743	-100	10.389	-	-	-	-	-	-	-	-	-	-	-	90	-
5-Cl 05	-	-	101	10.389	010	18.234	-	-	-	-	-	-	-	-	90	-	-
5-Cl 06	-	-	-	-	-	-	-	-	-	-	-	-	-	-	-	-	-
5-Cl 07	-	-	-	-	-	-	-	-	-	-	-	-	-	-	-	-	-
5-Cl 08	-	-	½-1.5 0	11.091	-	-	½ -½ 0	7.649	-	-	0-10	5.680	½-½ 0	7.649	-	-	68.21
5-Cl 09	-	-	-1-10	10.635	-	-	-	-	-	-	-100	5.664	0-10	7.634	-	-	74.75
5-Cl 10	-100	4.808	-101	10.104	0-10	19.471	-	-	-	-	-	-	-	-	90	90.28	-
5-Cl 11	-	-	110	10.444	-	-	-	-	-	-	100	5.617	010	7.527	-	-	75.72
5-Cl 12	-	-	½ 1.5 0	10.019	-	-	½ ½ 0	7.564	-	-	010	5.666	½ ½ 0	7.564	-	-	68.00
5-Cl β	-	-	-10-1	10.942	010	17.895	-	-	-	-	-	-	-	-	90	-	-
5-Cl α	010	4.714	-100	10.086	-	-	-	-	-	-	-	-	-	-	-	-	-
6-F	-	-	-	-	-	-	0-10	7.095	-	-	-	-	-	-	-	-	-
Asp 1	-	-	-	-	-	-	-	-	-	-	-	-	-	-	-	-	-
Asp 2	-	-	-	-	-	-	-	-	101	13.240	-	-	-	-	-	-	-

References

1. O. Lehmann, *Molekularphisik, Engelmann, Liepzig* **1888**, 193.
2. GADDS V4.1.32. Bruker AXS. Smith, K.L., Jin, Z., Chambers, L., He, B., Preckwinkel, U., Moran, D.
3. Bond, A. D.; Boese, R.; Desiraju, G. R., *Angew. Chem. Int. Edit.* **2007**, 46, 615.
4. Bond, A. D.; Boese, R.; Desiraju, G. R., *Angew. Chem. Int. Edit.* **2007**, 46, 618.
5. Bond, A. D.; Solanko, K. A.; Parsons, S.; Redder, S.; Boese, R., *CrystEngComm* **2011**, 13, 399.
6. Hursthouse, M. B.; Montis, R.; Tizzard, G. J., *CrystEngComm* **2011**, 13, 3390.